
Article:
Giunta, V., Hillen, T., Lewis, M. et al. (1 more author) (2022) Local and global existence for nonlocal multispecies advection-diffusion models. SIAM Journal on Applied Dynamical Systems, 21 (3). pp. 1686-1708. ISSN 1536-0040

https://doi.org/10.1137/21M1425992

Local and Global Existence for Non-local Multi-Species Advection-Diffusion Models *

Valeria Giunta†, Thomas Hillen ‡, Mark A. Lewis §, and Jonathan R. Potts†

Abstract. Non-local advection is a key process in a range of biological systems, from cells within individuals to the movement of whole organisms. Consequently, in recent years, there has been increasing attention on modelling non-local advection mathematically. These often take the form of partial differential equations, with integral terms modelling the non-locality. One common formalism is the aggregation-diffusion equation, a class of advection diffusion models with non-local advection. This was originally used to model a single population, but has recently been extended to the multi-species case to model the way organisms may alter their movement in the presence of coexistent species. Here we prove existence theorems for a class of non-local multi-species advection-diffusion models, with an arbitrary number of co-existent species. We prove global existence for models in $n = 1$ spatial dimension and local existence for $n > 1$. We describe an efficient spectral method for numerically solving these models and provide example simulation output. Overall, this helps provide a solid mathematical foundation for studying the effect of inter-species interactions on movement and space use.

Key words. Advection-diffusion, Aggregation-diffusion, Existence theorems, Mathematical ecology, Non-local advection, Taxis.

AMS subject classifications. 35A01, 35B09, 35B65, 35R09, 92-10, 92D40

1. Introduction.

It is essential for individuals, whether cells or animals, to gain information about their local environment [62, 56]. Not only do individuals sense environmental features, such as food, temperature, pH-level, and so on, they also are able to detect other individuals in a local spatial neighborhood, such as predators, prey, or conspecifics [19, 47]. This feature is not only restricted to higher level species, but is also found in cells [31]. For example human immune cells gather information about their tissue environment and they are able to distinguish friend from foe [58, 26]. The process of gaining information about presence or absence of other species in the environment is intrinsically non-local [16, 41]. Mathematically, the non-local sensing of neighboring individuals leads to non-local advection terms in the corresponding continuum models, and that is the topic of this paper.

Non-local advection is a mechanism underlying a wide range of biological systems. In ecology, animals sense their surroundings and make decisions to avoid predators, find prey,

*Submitted to the editors 09/06/2021.

Funding: VG and JRP acknowledge the support of an Engineering and Physical Sciences Research Council (EPSRC) grant EP/V002988/1 awarded to JRP. VG also acknowledges support from GNFM-INdAM and the Italian MIUR through project PRIN2017 2017YBKNCE. TH is grateful for support from the Natural Science and Engineering Council of Canada Discovery Grant RGPIN-2017-04158. MAL gratefully acknowledges support from the NSERC Discovery and Canada Research Chair programs.

†School of Mathematics and Statistics, University of Sheffield, Hicks Building, Hounsfield Road, Sheffield, S3 7RH, UK (v.giunta@sheffield.ac.uk, j.potts@sheffield.ac.uk).

‡Department of Mathematical and Statistical Sciences, University of Alberta, Edmonton T6G 2G1, Alberta, Canada (thillen@ualberta.ca).

§Department of Mathematical and Statistical Sciences and Department of Biological Sciences, University of Alberta, Edmonton T6G 2G1, Alberta, Canada (mark.lewis@ualberta.ca)

and/or aggregate in swarms, flocks or herds [16, 21, 27, 38, 44]. This non-local sensing can occur on several scales, from near to far [7, 4, 43]. These scales affect the overall spatial arrangement of populations [51, 14, 2] and can lead to species aggregation, segregation, and also more complex mixing patterns [27, 25, 54]. Whereas animals can sense and interact over distances using sight, smell and hearing, in cell biology, cells interact non-locally by extending long thin protrusions, probing the environment [2, 49, 48]. Chemotaxis processes, leading to the following of chemical trails by organisms, can also be formulated as non-local advective processes [33, 59], and have been observed in taxa from single-celled organisms to insect populations to large vertebrate animals [34].

From a mathematical modelling perspective, non-locality in continuum models often arises as an integral term inside a derivative. The corresponding models become intrinsically non-local, and classical theories, developed for local models, no longer apply [14, 17]. Non-local terms in continuum models offer new challenges and new opportunitites [6, 9, 53, 44, 14]. For example, in single-species models of aggregation, the structure of the non-local advective term is fundamental for avoiding blow-up and ensuring global existence of solutions [33, 23, 8, 17]. In models of home ranges [11] and territory formation [52], non-local advection is necessary for ensuring well-posedness. In the context of modelling swarm dynamics, [44] showed that non-local advection is vital for the formation of cohesive swarms.

Consequently, non-local advection has become a popular feature of biological models [14]. One common class of such models is the aggregation-diffusion equation [61, 22]. This models a single population, $u(x,t)$, that undergoes diffusion and non-local self-attractive advection, leading to the following general form [17]

$$\frac{\partial u}{\partial t} = \Delta u^m - \nabla \cdot [u \nabla (K * u)], \tag{1.1}$$

where $K * u$ is the convolution of u with a spatial averaging kernel, K, and m is a positive integer. As such, the structure of K models the non-local interactions of the population with itself. Equation (1.1) can lead to the spontaneous formation of non-uniform patterns, consisting of single or multiple stationary aggregations of various shapes and sizes, under certain conditions [35, 20]. However, there is numerical evidence that the multiple-aggregation case is often, and possibly always, metastable [61, 12, 17].

One can readily generalise the aggregation-diffusion equation to the multi-species situation as follows:

$$\frac{\partial u_i}{\partial t} = D_i \Delta u_i^m - \nabla \cdot \left[u_i \nabla \sum_{j=1}^{N} h_{ij} K * u_j \right], \tag{1.2}$$

where $u_1(x,t), \ldots, u_N(x,t)$ are locational densities of $N \geq 1$ populations at time t, $D_i \in \mathbb{R}_{>0}$ is the diffusion constant of population i, and $h_{ij} \in \mathbb{R}$ are constants denoting the attractive (if $h_{ij} > 0$) or repulsive (if $h_{ij} < 0$) tendencies of population i to population j. Indeed, the $N = 2$ case has received some attention [28, 18], with equations of the same or similar form to Equation (1.2) being applied to predator-prey dynamics [29], animal territoriality [52], cell-sorting [49] as well as human gangs [3]. For $N = 2$, it is possible to observe both aggregation and segregation patterns emerge, depending on the relative values of the h_{ij} constants [28, 54].

An example of Equation (1.2) where N is arbitrary was proposed by [54] as a model of animal ecosystems. The authors assumed that each population can detect the population density of other populations over a local spatial neighbourhood. The mechanism behind this detection could have various forms, three of which are explained in [54]: direct observations of individuals at a distance, indirect communication via marking the environment (e.g. using urine or faeces), and memory of past interactions with other populations. [54] showed that all three of these biological mechanisms lead to the same multi-species aggregation-diffusion model in the appropriate adiabatic limit. The authors analysed pattern formation properties of Equation (1.2) where the diffusion term is linear, i.e. $m = 1$, in one spatial dimension with periodic boundary conditions. They further assumed that $K(x)$ is a top-hat kernel, i.e. $K(x) = 1/(2\delta)$ for $x \in (-\delta, \delta)$ and $K(x) = 0$ otherwise, and also that $j \neq i$ (i.e. no self-attraction or repulsion). With these assumptions in place, the authors showed that, whilst the pattern formation properties when $N = 2$ can be fully categorised, the $N = 3$ case is much richer. Indeed, numerical analysis for $N = 3$ revealed stationary patterns, regular oscillations, period-doubling bifurcations, and irregular spatio-temporal patterns suggestive of chaos [54].

These insights highlighted the importance of understanding non-linear, non-local feedbacks between the locations of animal populations. In the ecological literature, the field of *Species Distribution Modelling* (SDM) is dominated by efforts to find correlations between animal locations and environmental features [1, 64]. These features are then used to predict species distributions in either new locations or future environmental conditions [5, 42] and hence inform conservation actions [63]. However, despite considerable research effort into SDMs, a recent meta-analysis of 33 different SDM approaches revealed that none of the models studied were good at making predictions in a range of novel situations [46]. Based on the results of [54], we conjecture that this may be, in part, due to a failure of these models to account for non-linear feedbacks in movement mechanisms. We propose that employing a multi-species aggregation-diffusion approach, typified by Equation (1.2), may help improve predictive performance when modelling the spatial distributions of animal populations.

As a step to this end, the aim of this paper is twofold: to begin building solid mathematical foundations underlying the model and observations of [54], and to construct an efficient numerical scheme for future investigations. For our mathematical analysis, we are able to drop the assumption from [54] that $j \neq i$, thus allowing for self attraction or repulsion. However, we have to assume that K is twice differentiable, so cannot be the same top-hat function used by [54] but can be a smooth approximation of the top-hat function. With these assumptions in place, we prove the global existence of a unique, positive solution in one spatial dimension and local existence (up to a finite time T_*) in arbitrary dimensions. We also propose an efficient scheme for solving multi-species aggregation-diffusion models numerically, based on a spectral method, and give some example output of both stationary and fluctuating patterns.

We focus here on the case of linear diffusion $m = 1$ in Equation (1.2). One reason is that linear diffusion models have been used with great success in biological modelling, and the common reaction-diffusion setting is a natural place to start ([45]). Also, the use of the heat equation semigroup is quite essential in our analysis. The general case for $m > 1$ has a more physical motivation, as it is based on an energy minimizing principle. Variational calculus can then be used to address the corresponding well-posedness problem [6, 12, 17].

Our paper is organised as follows. Section 2 introduces the study system and states

the main results (global existence and positivity in one spatial dimension; local existence in arbitrary dimensions). In Section 3 we prove the main results. Section 4 details a method for numerically solving the study system, together with some example numerical output. Section 5 gives a discussion and concluding remarks.

2. The Model. We consider N different populations of moving organisms. These could either be different species or different groups within a species, such as territorial groupings or herds. In either case, we use the term *population* and write $u_i(x,t)$ to denote the density of population $i \in \{1,...,N\}$ at time t. As with Equation (1.2), we assume that each population detects the population density of other populations over space, and adjusts its directed motion via advection towards a weighted sum of the spatially averaged population densities.

Before generalising to arbitrary dimensions, we first define our system in one dimension (1D) as follows

$$\frac{\partial u_i}{\partial t} = D_i \frac{\partial^2 u_i}{\partial x^2} - \frac{\partial}{\partial x}\left[u_i \frac{\partial}{\partial x}\left(\sum_{j=1}^{N} h_{ij}\bar{u}_j\right)\right],$$

$$\bar{u}_j(x) = (K * u_j)(x) := \int_0^L K(x-y)u_j(y)dy. \tag{2.1}$$

We examine this system on a domain $[0,L]$ with periodic boundary conditions, so that $\Omega = [0,L]/\{0,L\}$ (the topological quotient of $[0,L]$ by $\{0,L\}$). Here, $K \geq 0$ is a *local averaging kernel* (i.e. a probability density function on Ω with zero mean), D_i is the diffusion constant of population i, and h_{ij} is the strength of attraction (resp. repulsion) of population i to (resp. from) population j if $h_{ij} > 0$ (resp. $h_{ij} < 0$). The local averaging kernel, K, describes the spatial scale over which organisms scan the environment when deciding to move in response to the presence of other populations. Here, we will assume K is twice differentiable with $\nabla K \in L^\infty(\mathbb{T})$.

Notice that $\int_\Omega u_i(x,t)dx$ does not vary over time so we define a constant $p_i = \int_\Omega u_i(x,t)dx$ for each i. Consequently, our model is suitable for modelling systems of animal or cell populations over timescales where births and deaths have a negligible effect on the population size. For example, for systems of organisms whose population sizes vary by only small amounts across a season (as is the case for many mammals, birds, and reptiles in summer), this could model dynamics over a single season.

We can use vector notation to write System (2.1) in a more compact form. Let

$$u = (u_1, \dots u_N)^T, \qquad D = \mathrm{diag}(D_1, \dots, D_N), \qquad H = (h_{ij})_{i,j},$$

where $(h_{ij})_{i,j}$ denotes the matrix whose i,j-th entry is h_{ij}. Then System (2.1) can be written as

$$u_t = Du_{xx} - (u \cdot (H\bar{u})_x)_x. \tag{2.2}$$

In higher dimensions we make the analogous assumption that $\Omega \subset \mathbb{R}^n$ is a periodic domain, i.e. a torus $\mathbb{T}$. Then the system on the general n-dimensional torus $\mathbb{T}$ becomes

$$u_t = D\Delta u - \nabla \cdot (u \cdot \nabla(H\bar{u})). \tag{2.3}$$

To avoid confusion in this vector notation we can write each row as

$$u_{it} = D_i \sum_k \frac{\partial^2}{\partial x_k^2} u_i - \sum_k \frac{\partial}{\partial x_k} \left(u_i \sum_j \frac{\partial}{\partial x_k} (h_{ij}\bar{u}_j) \right),$$

which leads to

$$u_t = D \sum_k \frac{\partial^2}{\partial x_k^2} u - \sum_k \frac{\partial}{\partial x_k} \left(u \circ \sum_j \frac{\partial}{\partial x_k} (H_{\cdot j}\bar{u}_j) \right),$$

where $H_{\cdot j}$ is the j-th column of H and $\circ$ is the Hadamard product. We now state our main result, as follows.

Theorem 2.1. *Assume $u_0 \in H^2(\mathbb{T})^N$ and K is twice differentiable. If $n \geq 1$ then there exists a time $T_* \in (0, \infty]$ and a unique solution u to Equation (2.3), valid for $t \in [0, T_*)$, such that*

$$u \in C^1((0, T_*), L^2(\mathbb{T}))^N \cap C^0([0, T_*), H^2(\mathbb{T}))^N.$$

If $n = 1$ and $u_0 \in C^2(\mathbb{T})^N$ such that $u_0(x) > 0$ for $x \in \mathbb{T}$, then there is a unique positive solution u to Equation (2.3) such that

$$u \in C^1((0, \infty), L^2(\mathbb{T}))^N \cap C^0([0, \infty), C^2(\mathbb{T}))^N.$$

The first part of this theorem ($n \geq 1$) will follow from Lemma 3.8 and does not require a non-negative initial data. The second ($n = 1$) will be established in Theorem 3.10.

2.1. Notation. We will employ the following notation throughout. Let $f : L^p(\Omega) \to \mathbb{R}$.

- $\|f\|_{L_p} = (\int_\Omega |f|^p)^{1/p}$, where $1 \leq p < \infty$.
- $\|f\|_{L^\infty} = inf\{C \geq 0 : |f(x)| \leq C, a.e.\}$.

Let $g = (g_1, g_2, \ldots, g_N) : (L^p)^N \to \mathbb{R}$. We will use the following norms

- $\|g\|_{(L_p)^N} = \sum_{i=1}^N \|g_i\|_{L^p}$, where $1 \leq p < \infty$.
- $\|g\|_{(L^\infty)^N} = \max_{i=1,2,\ldots,N}\{\|g_i\|_{L^\infty}\}$.

To ease the notation, we will usually omit the index N and write $\|g\|_{L^p}$ instead of $\|g\|_{(L^p)^N}$.

3. Model Analysis.

3.1. Existence and uniqueness of mild solutions.

Definition 3.1. *Given $u_0 \in (L^2(\mathbb{T}))^N$ and $T > 0$. We say that*

$$u(x, t) \in L^\infty((0, T), L^2(\mathbb{T}))^N$$

is a mild solution of Equation (2.3) if

$$u = e^{D\Delta t} u_0 - \int_0^t e^{D\Delta(t-s)} \nabla \cdot (u \cdot \nabla(H\bar{u}))ds, \tag{3.1}$$

for each $0 < t \leq T$, where $e^{D\Delta t}$ denotes the solution semigroup of the heat equation system $u_t = D\Delta u$ on $\mathbb{T}$, i.e. on Ω with periodic boundary conditions.

The crucial term in (2.2) is the non-local term $H\bar{u}$ and the following a-priori estimates for $\bar{u}$ are essential for the existence theory of this model. We will consider convolution with an appropriately smooth kernel, K. Eventually, in Lemma 3.4, we will need to assume that K is twice differentiable, but the first two Lemmas only require K to be (once) differentiable, so we state them in this more general case.

Lemma 3.2. *Let $\varphi \in L^2(\mathbb{T})$ and $K : \mathbb{T} \to \mathbb{R}$ be differentiable. Then $\|\bar{\varphi}\|_{H^1} = \|K * \varphi\|_{H^1} \leq (\|K\|_{L^1} + \|\nabla K\|_{L^1})\|\varphi\|_{L^2}$.*

Proof. First, $\|K * \varphi\|_{H^1} = \|K * \varphi\|_{L^2} + \|\nabla(K * \varphi)\|_{L^2}$. We also observe that $\nabla(K * \varphi) = \nabla K * \varphi = (\partial_{x_1} K * \varphi, \partial_{x_2} K * \varphi, \ldots, \partial_{x_n} K * \varphi)$. Then, applying Young's convolution inequality to both summands, we have $\|K * \varphi\|_{L^2} \leq \|K\|_{L^1}\|\varphi\|_{L^2}$ and $\|\nabla(K * \varphi)\|_{L^2} = \|(\nabla K) * \varphi\|_{L^2} = \|(\partial_{x_1} K * \varphi, \partial_{x_2} K * \varphi, \ldots, \partial_{x_n} K * \varphi)\|_{L^2} = \sum_{i=1}^n \|\partial_{x_i} K * \varphi\|_{L^2} \leq \sum_{i=1}^n \|\partial_{x_i} K\|_{L^1}\|\varphi\|_{L^2} = \|\nabla K\|_{L^1}\|\varphi\|_{L^2}$, proving the lemma. ∎

Lemma 3.3. *Let $\varphi \in L^\infty(\mathbb{T})$ and $K : \mathbb{T} \to \mathbb{R}$ be differentiable with $\nabla K \in L^\infty(\mathbb{T})$. Then $\|\nabla K * \varphi\|_{L^\infty} \leq |\mathbb{T}|^{1/2}\|\nabla K\|_{L^\infty}\|\varphi\|_{L^2}$.*

Proof. First note that

$$\begin{aligned}
\|\nabla(K * \varphi)\|_{L^\infty} &= \|(\nabla K) * \varphi\|_{L^\infty} \\
&= \|(\partial_{x_1} K * \varphi, \partial_{x_2} K * \varphi, \ldots, \partial_{x_n} K * \varphi)\|_{L^\infty} \\
&= \max_{i=1,2,\ldots,n} \{\|\partial_{x_i} K * \varphi\|_{L^\infty}\} \\
&\leq \max_{i=1,2,\ldots,n} \{\|\partial_{x_i} K\|_{L^\infty}\|\varphi\|_{L^1}\} \\
&= \max_{i=1,2,\ldots,n} \{\|\partial_{x_i} K\|_{L^\infty}\}\|\varphi\|_{L^1} \\
&= \|\nabla K\|_{L^\infty}\|\varphi\|_{L^1},
\end{aligned}$$

using Young's convolution inequality in the fourth line. Then, since $\mathbb{T}$ is of finite measure in $\mathbb{R}^N$, we have $\|\varphi\|_{L^1} \leq |\mathbb{T}|^{1/2}\|\varphi\|_{L^2}$ (this step uses Hölder's inequality, applied to $\|\mathbf{1}\varphi\|_{L^1}$ where $\mathbf{1} : \mathbb{T} \to \mathbb{R}$ such that $\mathbf{1}(x) = 1$). Hence $\|\nabla K\|_{L^\infty}\|\varphi\|_{L^1} \leq |\mathbb{T}|^{1/2}\|\nabla K\|_{L^\infty}\|\varphi\|_{L^2}$, proving the lemma. ∎

Lemma 3.4. *Let $\varphi \in H^1(\mathbb{T})$ and $K : \mathbb{T} \to \mathbb{R}$ be twice differentiable with $\nabla K \in L^\infty(\mathbb{T})$. Then $\|\Delta(K * \varphi)\|_{L^\infty} \leq \|\nabla K\|_{L^\infty}\|\nabla\varphi\|_{L^2}|\mathbb{T}|^{1/2}$.*

Proof. First note that

$$\begin{aligned}
\|\Delta(K * \varphi)\|_{L^\infty} &= \left\| \sum_{i=1}^n \partial_{x_i}^2 (K * \varphi) \right\|_{L^\infty} \\
&= \left\| \sum_{i=1}^n \partial_{x_i} K * \partial_{x_i}\varphi \right\|_{L^\infty} \\
&\leq \sum_{i=1}^n \|\partial_{x_i} K * \partial_{x_i}\varphi\|_{L^\infty}
\end{aligned}$$

$$\leq \sum_{i=1}^{n} \|\partial_{x_i} K\|_{L^\infty} \|\partial_{x_i} \varphi\|_{L^1}$$
$$\leq \|\nabla K\|_{L^\infty} \|\nabla \varphi\|_{L^1},$$

where the second inequality uses Young's convolution inequality. Then, as in Lemma 3.3, we have $\|\nabla\varphi\|_{L^1} \leq |\mathbb{T}|^{1/2}\|\nabla\varphi\|_{L^2}$. Hence $\|\nabla K\|_{L^\infty}\|\nabla\varphi\|_{L^1} \leq |\mathbb{T}|^{1/2}\|\nabla K\|_{L^\infty}\|\nabla\varphi\|_{L^2}$, proving the lemma. ∎

Before we formulate the proof of local and global existence, we recall a regularity result for the heat equation semigroup on a torus as formulated by [60] p.274:

Lemma 3.5. *For all $p \geq q > 0$ and $s \geq r$ we have the embedding*

$$e^{\Delta t} : W^{r,q}(\mathbb{T}) \to W^{s,p}(\mathbb{T}), \qquad \text{with norm } Ct^{-\kappa},$$

where C is a constant and

$$\kappa = \frac{n}{2}\left(\frac{1}{q} - \frac{1}{p}\right) + \frac{1}{2}(s - r).$$

Theorem 3.6. *For each $u_0 \in L^2(\mathbb{T})^N$, if K is differentiable then there exists a time $T > 0$ and a unique mild solution (3.1) of Equation (2.3) with*

$$u \in L^\infty((0,T), L^2(\mathbb{T}))^N.$$

Proof. The proof uses a Banach fixed-point argument. Let $M := 2\|u_0\|_{L^2}$. We define a map

$$v \mapsto Qv := e^{D\Delta t}u_0 - \int_0^t e^{D\Delta(t-s)}\nabla \cdot (v \cdot \nabla(H\bar{v}))ds,$$

for $v \in L^\infty((0,T), L^2(\mathbb{T}))^N$.

Step 1: Q maps a ball into itself: Let $B_M(0) \subset L^2(\mathbb{T})^N$ be the ball of radius M in $L^2(\mathbb{T})^N$. Let $v = (v_1, \ldots, v_N) \in L^\infty((0, T_{min}), B_M(0))^N$, where T_{min} will be determined later. Writing $u_0 = (u_{10}, ..., u_{N0})$, for each $T \in (0, T_{min})$ we have

$$\|Qv_i\|_{L^2} \leq \|u_{i0}\|_{L^2} + \left\| \int_0^T e^{D\Delta(T-s)}\nabla \cdot (v_i \nabla((H\bar{v})_i))ds \right\|_{L^2}$$
$$\leq \|u_{i0}\|_{L^2} + \int_0^T C(T-s)^{-\frac{1}{2}}\|v_i\nabla((H\bar{v})_i)\|_{L^2}ds$$
$$\leq \|u_{i0}\|_{L^2} + 2C\sqrt{T}\sup_{0<t\leq T}\|v_i\nabla((H\bar{v})_i)\|_{L^2}.$$

In the second inequality we used the regularizing property of the heat equation semigroup from H^{-1} to L^2 with a norm $Ct^{-\frac{1}{2}}$, as in Lemma 3.5. Since $(H\bar{v})_i = \sum_{j=1}^N h_{ij}K * v_j$, we

continue the previous estimate as:

$$\begin{aligned}
\|Qv_i\|_{L^2} &\leq \|u_{i0}\|_{L^2} + 2C\sqrt{T} \sup_{0<t\leq T} \left\| v_i \nabla \left(\sum_{j=1}^{N} h_{ij} K * v_j \right) \right\|_{L^2} \\
&\leq \|u_{i0}\|_{L^2} + 2C\sqrt{T} \sup_{0<t\leq T} \sum_{j=1}^{N} |h_{ij}| \, \|v_i \nabla (K * v_j)\|_{L^2} \\
&\leq \|u_{i0}\|_{L^2} + 2C\sqrt{T} \sum_{j=1}^{N} |h_{ij}| \sup_{0<t\leq T} n\|v_i\|_{L^2} \, \|\nabla (K * v_j)\|_{L^\infty} \\
&\leq \|u_{i0}\|_{L^2} + 2C\sqrt{T} \|\nabla K\|_{L^\infty} |\mathbb{T}|^{1/2} \sum_{j=1}^{N} |h_{ij}| \sup_{0<t\leq T} n\|v_i\|_{L^2} \|v_j\|_{L^2}
\end{aligned}$$

In the third inequality we used Hölder's inequality, and in the last one we used Lemma 3.3. From the previous estimate, we obtain

$$\begin{aligned}
\|Qv\|_{L^2} &= \sum_{i=1}^{N} \|Qv_i\|_{L^2} \\
&\leq \sum_{i=1}^{N} \|u_{i0}\|_{L^2} + 2C\sqrt{T} n |\mathbb{T}|^{1/2} \|\nabla K\|_{L^\infty} \sum_{i,j=1}^{N} |h_{ij}| \sup_{0<t\leq T} \|v_i\|_{L^2} \|v_j\|_{L^2} \\
&\leq \|u_0\|_{L^2} + 2C\sqrt{T} n |\mathbb{T}|^{1/2} \|\nabla K\|_{L^\infty} \|H\|_\infty \sup_{0<t\leq T} \|v\|_{L^2}^2,
\end{aligned}$$

where $\|H\|_\infty = \max_{i,j} |h_{ij}|$. Notice that $\|u_0\|_{L^2} = \frac{M}{2}$, hence we can always find a time T_1 small enough such that

$$\sup_{0<t\leq T_1} \|Qv\|_{L^2} \leq M,$$

so that $Qv \in L^\infty((0,T_1), B_M(0))^N$.

Step 2: Q is a contraction for T small enough: Given $v_1 = (v_{11}, ..., v_{1N}), v_2 = (v_{21}, ..., v_{2N}) \in$

$L^\infty((0,T_{min}),B_M(0))^N$, we compute for $T\in(0,T_{min})$ the following

$$
\begin{aligned}
\|Qv_{1i}-Qv_{2i}\|_{L^2} &= \left\| \int_0^T e^{D\Delta(T-s)}\left[\nabla\cdot(v_{1i}\nabla((H\bar v_1)_i))-\nabla\cdot(v_{2i}\nabla((H\bar v_2)_i))\right]ds\right\|_{L^2}\\
&\le \left\| \int_0^T e^{D\Delta(T-s)}\nabla\cdot((v_{1i}-v_{2i})\nabla((H\bar v_1)_i)ds\right\|_{L^2}\\
&\quad+\left\| \int_0^T e^{D\Delta(T-s)}\nabla\cdot[v_{2i}\nabla(H(\bar v_{1i}-\bar v_{2i}))_i]ds\right\|_{L^2}\\
&\le \int_0^T C(T-s)^{-1/2}\|(v_{1i}-v_{2i})\nabla((H\bar v_1)_i)\|_{L^2}ds\\
&\quad+\int_0^T C(T-s)^{-1/2}\|v_{2i}\nabla((H(\bar v_1-\bar v_2))_i)\|_{L^2}ds\\
&\le 2C\sqrt{T}\sup_{0<t\le T}(\|(v_{1i}-v_{2i})\nabla((H\bar v_1)_i)\|_{L^2}+\|v_{2i}\nabla((H(\bar v_1-\bar v_2))_i)\|_{L^2})
\end{aligned}
$$

In the second inequality we used the regularizing property of the heat equation semigroup from H^{-1} to L^2 with a norm $Ct^{-\frac{1}{2}}$, as in Lemma 3.5. Since $(H\bar v_1)_i=\sum_{j=1}^N h_{ij}K*v_{1j}$ and $(H\bar v_2)_i=\sum_{j=1}^N h_{ij}K*v_{2j}$ we continue the previous estimate as:

$$
\begin{aligned}
\|Qv_{1i}-Qv_{2i}\|_{L^2} &\le 2C\sqrt{T}\sup_{0<t\le T}\left(\left\|(v_{1i}-v_{2i})\sum_{j=1}^N|h_{ij}|(\nabla K*\ v_{1j})\right\|_{L^2}\right.\\
&\quad\left.+\left\|v_{2i}\sum_{j=1}^N|h_{ij}|(\nabla K*(v_{1j}-v_{2j}))\right\|_{L^2}\right)\\
&\le 2C\sqrt{T}\sup_{0<t\le T}(\|v_{1i}-v_{2i}\|_{L^2}n\sum_{j=1}^N|h_{ij}|\|\nabla K*\ v_{1j}\|_{L^\infty}\\
&\quad+\|v_{2i}\|_{L^2}n\sum_{j=1}^N|h_{ij}|\|\nabla K*(v_{1j}-v_{2j})\|_{L^\infty})\\
&\le 2C\sqrt{T}\|H\|_\infty\|\nabla K\|_{L^\infty}|\mathbb{T}|^{1/2}n\sup_{0<t\le T}\left(\|v_{1i}-v_{2i}\|_{L^2}\sum_{j=1}^N\|v_{1j}\|_{L^2}\right.\\
&\quad\left.+\|v_{2i}\|_{L^2}\sum_{j=1}^N\|v_{1j}-v_{2j}\|_{L^2}\right),
\end{aligned}
$$

where $\|H\|_\infty=\max_{i,j}|h_{ij}|$. In the second inequality we used Hölder's inequality, and in the

last one we used Lemma 3.3. From the previous estimate, we obtain

$$\begin{aligned}
\|Qv_1 - Qv_2\|_{L^2} &= \sum_{i=1}^{N} \|Qv_{1i} - Qv_{2i}\|_{L^2} \\
&\leq 2C\sqrt{T}\|H\|_\infty \|\nabla K\|_{L^\infty} |\mathbb{T}|^{1/2} n \sup_{0<t\leq T} \left(\sum_{i=1}^{N} \|v_{1i} - v_{2i}\|_{L^2} \sum_{j=1}^{N} \|v_{1j}\|_{L^2} \right. \\
&\qquad \left. + \sum_{i=1}^{N} \|v_{2i}\|_{L^2} \sum_{j=1}^{N} \|v_{1j} - v_{2j}\|_{L^2} \right) \\
&\leq 2C\sqrt{T}\|H\|_\infty \|\nabla K\|_{L^\infty} |\mathbb{T}|^{1/2} n \sup_{0<t\leq T} (\|v_1 - v_2\|_{L^2}(\|v_1\|_{L^2} + \|v_1\|_{L^2})) \\
&\leq 4MC\sqrt{T}\|H\|_\infty \|\nabla K\|_{L^\infty} |\mathbb{T}|^{1/2} n \sup_{0<t\leq T} \|v_1 - v_2\|_{L^2}.
\end{aligned}$$

The last inequality is obtained from $v_1, v_2 \in L^\infty((0, T_{min}), B_M(0))^N$, so $\|v_1\|_{L^2}, \|v_2\|_{L^2} \leq M$. For

$$T < T_2 := \frac{1}{|\mathbb{T}|(4MCn\|H\|_\infty \|\nabla K\|_{L^\infty})^2}$$

we have

$$\sup_{0<t\leq T} \|Qv_1 - Qv_2\|_{L^2} < \sup_{0<t\leq T} \|v_1 - v_2\|_{L^2},$$

which means $Qv_1 - Qv_2 \in L^\infty((0, T_2), B_M(0))^N$. Thus Q is a strict contraction in $L^\infty((0, T_{min}), B_M(0))^N$, where we can finally define T_{min} as

$$T_{min} := \min\{T_1, T_2\}.$$

Step 3: The previous argument also shows that Q is Lipschitz continuous, hence, by the Banach fixed point theorem, Q has a unique fixed point for $T < T_{min}$. This fixed point is a mild solution of (2.2) and it satisfies

$$u \in L^\infty((0, T), L^2(\mathbb{T}))^N$$

for $T < T_{min}$. The mild solution automatically satisfies the initial condition:

$$\lim_{t\to 0} u(x, t) = u_0(x).$$

3.2. Global existence in time.

Let u be a mild solution of Equation (2.3). Our strategy moving forward will be to show that, for the period of time that $\|u\|_{L^1}$ remains bounded, solutions exist and grow at most exponentially in L^2. We will then show that the statement '$\|u\|_{L^1}$ is unbounded' leads to a contradiction.

With this in mind, we define a time T_* as follows: if $\|u\|_{L^1}$ is bounded for all time, then let $T_* = \infty$. Otherwise, $\|u\|_{L^1} \to \infty$ as $t \to T_{max}$ for some $T_{max} \in (0, \infty]$, so let T_* be the earliest time at which $\|u\|_{L^1} = 2\|u_0\|_{L^1}$. Our objective will be to show that the case where $\|u\|_{L^1} \to \infty$ as $t \to T_{max}$ leads to a contradiction when $n = 1$ (one spatial dimension), so that $\|u\|_{L^1}$ is bounded for all time. This will enable us to prove that the solution from Theorem 3.6 is global in time when $n = 1$.

Lemma 3.7. *Let $u = (u_1, \dots, u_N)$ be a mild solution and $K : \mathbb{T} \to \mathbb{R}$ be differentiable with $\nabla K \in L^\infty(\mathbb{T})$. Then there exists a constant ν_i such that $\|\nabla(\mathcal{K} * u_i)\|_{L^\infty} \le \nu_i$ for all $t < T_*$, $i \in \{1, \dots, N\}$. If $\nu = \nu_1 + \cdots + \nu_N$ then $\|\nabla(\mathcal{K} * u)\|_{L^\infty} \le \nu$.*

Proof. Applying Young's convolution inequality, we have $\|\nabla(\mathcal{K} * u_i)\|_{L^\infty} \le \|\nabla\mathcal{K}\|_{L^\infty}\|u_i\|_{L^1}$. By the definition of T_*, $\|u_i\|_{L^1}(t)$ is bounded for $t < T_*$. Thus there exists a constant ν_i such that $\|\nabla\mathcal{K}\|_{L^\infty}\|u_i\|_{L^1} \le \nu_i$. The result $\|\nabla(\mathcal{K} * u)\|_{L^\infty} \le \nu$ follows from the definitions of ν and the norm on $(L_1)^N$. ∎

Lemma 3.8. *Assume $u_0 \in H^2(\mathbb{T})^N$ and K is twice differentiable. Then the mild solution from Theorem 3.6 satisfies*

$$u \in C^1((0, T_*), L^2(\mathbb{T}))^N \cap C^0([0, T_*), H^2(\mathbb{T}))^N$$

In one spatial dimension this implies

$$u \in C^1((0, T_*), L^2(\mathbb{T}))^N \cap C^0([0, T_*), C^2(\mathbb{T}))^N,$$

and mild solutions are classical up to time T_*.

Proof. As we are dealing with a system of equations $u = (u_1, \dots, u_N)$, we consider each component separately. For each of the components u_i for $i = 1, \dots, N$ we multiply the i-th row of Equation (2.3) by u_i and integrate:

$$\begin{aligned}
\frac{1}{2}\frac{d}{dt}\|u_i\|_{L^2}^2 &= \int_{\mathbb{T}} u_i u_{it} dx \\
&= \int_{\mathbb{T}} D_i u_i \Delta u_i dx - \int_{\mathbb{T}} u_i \nabla \cdot (u_i \nabla((H\bar{u})_i)) dx \\
&= -\int_{\mathbb{T}} D_i |\nabla u_i|^2 dx + \int_{\mathbb{T}} u_i \nabla u_i \cdot \nabla((H\bar{u})_i) dx \\
&= -\int_{\mathbb{T}} D_i \sum_{h=1}^{n} (\partial_{x_h} u_i)^2 dx + \int_{\mathbb{T}} u_i \sum_{h=1}^{n} (\partial_{x_h} u_i)\partial_{x_h}((H\bar{u})_i) dx \\
&\le \sum_{h=1}^{n} \left(-\int_{\mathbb{T}} D_i (\partial_{x_h} u_i)^2 dx + \|\partial_{x_h}((H\bar{u})_i)\|_{L^\infty} \int_{\mathbb{T}} |u_i \partial_{x_h} u_i| dx \right) \\
&= -\int_{\mathbb{T}} D_i |\nabla u_i|^2 dx + \|\nabla((H\bar{u})_i)\|_{L^\infty} \int_{\mathbb{T}} |u_i \nabla u_i| dx \\
&= -\int_{\mathbb{T}} D_i |\nabla u_i|^2 dx + \|\sum_{j=1}^{N} h_{ij} \nabla(K * u_j)\|_{L^\infty} \int_{\mathbb{T}} |u_i \nabla u_i| dx \\
&\le -\int_{\mathbb{T}} D_i |\nabla u_i|^2 dx + \|H\|_\infty \sum_{j=1}^{N} \|\nabla(K * u_j)\|_{L^\infty} \int_{\mathbb{T}} |u_i \nabla u_i| dx
\end{aligned}$$

$$\leq -\int_{\mathbb{T}} D_i \left|\nabla u_i\right|^2 dx + \|H\|_\infty \nu \int_{\mathbb{T}} |u_i \nabla u_i| dx$$
$$\leq \left(-D_i + \frac{\varepsilon}{2}\left(\|H\|_\infty \nu\right)^2\right) \int_{\mathbb{T}} \left|\nabla u_i\right|^2 dx + \frac{n}{2\varepsilon} \int_{\mathbb{T}} |u_i|^2 dx$$

where $\|H\|_\infty = \max_{i,j} |h_{i,j}|$. In the third equality we used integration by parts and the periodic boundary conditions, the first inequality uses Hölder's inequality, the third inequality uses Lemma 3.7, which is valid for $t < T_*$, and the fourth inequality uses Young's inequality.

Now we choose ε such that $-D_i + \frac{\varepsilon}{2}\left(\|H\|_\infty \nu\right)^2 < 0$ for all $i, j = 1, \ldots, N$ so that

$$\frac{1}{2}\frac{d}{dt}\|u_i\|_{L^2}^2 \leq \frac{n}{2\varepsilon}\|u_i\|_{L^2}^2.$$

Applying Grönwall's Lemma, we find

$$\|u_i\|_{L^2} \leq \|u_{i0}\|_{L^2} e^{\frac{nt}{2\varepsilon}}.$$

Finally, we observe that

$$\sum_{i=1}^{N} \|u_i\|_{L^2} \leq \sum_{i=1}^{N} \|u_{i0}\|_{L^2} e^{\frac{nt}{2\varepsilon}},$$

from which we obtain

$$\|u\|_{L^2} \leq \|u_0\|_{L^2} e^{\frac{nt}{2\varepsilon}}. \tag{3.2}$$

Hence solutions exist and grow at most exponentially in L^2 up to time T_*.

Now we find an estimate in H^1 for each component u_i, $i = 1, \ldots, N$:

$$\frac{1}{2}\frac{d}{dt}\|\nabla u_i\|_{L^2}^2 = -\int_{\mathbb{T}} (\nabla u_{it}) \cdot (\nabla u_i) dx$$
$$= -\int_{\mathbb{T}} u_{it} \Delta u_i dx$$
$$= -\int_{\mathbb{T}} D_i (\Delta u_i)^2 dx + \int_{\mathbb{T}} \Delta u_i \nabla \cdot (u_i \nabla((H\bar{u})_i)) dx$$
$$= \left(-D_i + \frac{\varepsilon_2}{2}\right) \int_{\mathbb{T}} (\Delta u_i)^2 dx + \frac{1}{2\varepsilon_2} \int_{\mathbb{T}} (\nabla \cdot (u_i \nabla((H\bar{u})_i)))^2 dx,$$

where we used Young's inequality to obtain the last estimate. We now chose $\varepsilon_2 > 0$ small enough such that $-D_i + \frac{\varepsilon_2}{2} < 0$ for every $i = 1, \ldots, N$. We then continue the previous estimate

as

$$
\begin{aligned}
\frac{1}{2}\frac{d}{dt}\|\nabla u_i\|_{L^2}^2 &\le \frac{1}{2\varepsilon_2}\|\nabla\cdot(u_i\nabla((H\bar{u})_i))\|_{L^2}^2\\
&= \frac{1}{2\varepsilon_2}\left\|\sum_{h=1}^{n}\partial_{x_h}\left(u_i\partial_{x_h}\sum_{j=1}^{N}h_{ij}K*u_j\right)\right\|_{L^2}^2\\
&\le \frac{1}{2\varepsilon_2}\left\|\sum_{h=1}^{n}(\partial_{x_h}u_i)\partial_{x_h}\sum_{j=1}^{N}h_{ij}K*u_j+\sum_{h=1}^{n}u_i\partial_{x_h}^2\sum_{j=1}^{N}h_{ij}K*u_j\right\|_{L^2}^2\\
&\le \frac{1}{2\varepsilon_2}\left(\left\|\sum_{h=1}^{n}(\partial_{x_h}u_i)\partial_{x_h}\sum_{j=1}^{N}h_{ij}K*u_j\right\|_{L^2}+\left\|\sum_{h=1}^{n}u_i\partial_{x_h}^2\sum_{j=1}^{N}h_{ij}K*u_j\right\|_{L^2}\right)^2\\
&\le \frac{1}{\varepsilon_2}\left(\left\|\sum_{h=1}^{n}(\partial_{x_h}u_i)\partial_{x_h}\sum_{j=1}^{N}h_{ij}K*u_j\right\|_{L^2}^2+\left\|\sum_{h=1}^{n}u_i\partial_{x_h}^2\sum_{j=1}^{N}h_{ij}K*u_j\right\|_{L^2}^2\right)\\
&\le \frac{1}{\varepsilon_2}\left(\sum_{h=1}^{n}\|\partial_{x_h}u_i\|_{L^2}\sum_{j=1}^{N}|h_{ij}|\|\partial_{x_h}(K*u_j)\|_{L^\infty}\right)^2\\
&\quad+\frac{1}{\varepsilon_2}\left(\|u_i\|_{L^2}\sum_{j=1}^{N}\sum_{h=1}^{n}|h_{ij}|\|\partial_{x_h}^2(K*u_j)\|_{L^\infty}\right)^2\\
&\le \frac{1}{\varepsilon_2}\left(\|\nabla u_i\|_{L^2}\|H\|_\infty\sum_{j=1}^{N}\|\nabla(K*u_j)\|_{L^\infty}\right)^2\\
&\quad+\frac{1}{\varepsilon_2}\left(\|u_i\|_{L^2}\|H\|_\infty\sum_{h=1}^{n}\sum_{j=1}^{N}\|(\partial_{x_h}K)*(\partial_{x_h}u_j)\|_{L^\infty}\right)^2\\
&\le \frac{1}{\varepsilon_2}\left(\|\nabla u_i\|_{L^2}\|H\|_\infty\sum_{j=1}^{N}\|\nabla K\|_{L^\infty}\|u_j\|_{L^2}|\mathbb{T}|^{1/2}\right)^2\\
&\quad+\frac{1}{\varepsilon_2}\left(\|u_i\|_{L^2}\|H\|_\infty\sum_{h=1}^{n}\sum_{j=1}^{N}\|\partial_{x_h}K\|_{L^\infty}\|\partial_{x_h}u_j\|_{L^1}\right)^2\\
&\le \frac{1}{\varepsilon_2}\left(\|\nabla u_i\|_{L^2}\|H\|_\infty|\mathbb{T}|^{1/2}\sum_{j=1}^{N}\|\nabla K\|_{L^\infty}\|u_j\|_{L^2}\right)^2\\
&\quad+\frac{1}{\varepsilon_2}\left(\|u_i\|_{L^2}\|H\|_\infty|\mathbb{T}|^{1/2}\sum_{j=1}^{N}\|\nabla K\|_{L^\infty}\|\nabla u_j\|_{L^2}\right)^2\\
&\le \frac{1}{\varepsilon_2}\|H\|_\infty^2|\mathbb{T}|\|\nabla K\|_{L^\infty}^2\left(\|\nabla u_i\|_{L^2}^2\left(\sum_{j=1}^{N}\|u_j\|_{L^2}\right)^2+\|u_i\|_{L^2}^2\left(\sum_{j=1}^{N}\|\nabla u_j\|_{L^2}\right)^2\right)\\
&\le \frac{N}{\varepsilon_2}\|H\|_\infty^2|\mathbb{T}|\|\nabla K\|_{L^\infty}^2\left(\|\nabla u_i\|_{L^2}^2\sum_{j=1}^{N}\|u_j\|_{L^2}^2+\|u_i\|_{L^2}^2\sum_{j=1}^{N}\|\nabla u_j\|_{L^2}^2\right),
\end{aligned}
$$

in which we have used Young's inequality in the fourth inequality, Lemma 3.3 in the seventh, Lemma 3.4 in the eighth, and Young's inequality in the ninth.

Taking the sum over all the components $i \in \{1, \dots, N\}$, we have

$$\frac{1}{2}\frac{d}{dt}\sum_{i=1}^{N}\|\nabla u_i\|_{L^2}^2 \leq \frac{2N}{\varepsilon_2}\|H\|_\infty^2|\mathbb{T}|\|\nabla K\|_{L^\infty}^2\sum_{i=1}^{N}\|\nabla u_i\|_{L^2}^2\sum_{j=1}^{N}\|u_j\|_{L^2}^2.$$

By defining

$$A = \frac{4N}{\varepsilon_2}\|H\|_\infty^2|\mathbb{T}|\|\nabla K\|_{L^\infty}^2\sum_{j=1}^{N}\|u_{0j}\|_{L^2}^2,$$

and using (3.2), we arrive at

$$\frac{1}{2}\frac{d}{dt}\sum_{i=1}^{N}\|\nabla u_i\|_{L^2}^2 \leq \frac{A}{2}e^{\frac{nt}{2\varepsilon}}\sum_{i=1}^{N}\|\nabla u_i\|_{L^2}^2.$$

Applying Grönwall's Lemma, we have

$$\sum_{i=1}^{N}\|\nabla u_i\|_{L^2}^2(t) \leq \sum_{i=1}^{N}\|\nabla u_{i0}\|_{L^2}^2\exp\left(A\int_0^t\exp\left(\frac{ns}{2\varepsilon}\right)ds\right),$$

for each time $t < T_*$. Thus solutions remain bounded in $H^1(\mathbb{T})$ until time T_*.

Now let us consider the claim:

$$u \in \underbrace{C^1((0,T_*),L^2(\mathbb{T}))^N}_{(I)} \cap \underbrace{C^0([0,T_*),H^2(\mathbb{T}))^N}_{(II)}.$$

Looking again at the mild formulation in Equation (3.1), we have that $u \in H^1$, $\nabla(H\bar{u}) \in H^1$ and the integral term is in H^1. The first term involves the heat equation semigroup and the initial condition, and by the classical theory of the linear heat equation, the term $e^{D\Delta t}u_0$ is in H^1 and differentiable in time. Hence also u_t exists and is in L^2. This explains (I). Finally, writing down the equation once more:

$$u_t = D\Delta u - \nabla\cdot(u\nabla\cdot(H\bar{u}))$$

we now know that u_t is in L^2 and the non-local term as well. Hence $\Delta u \in L^2$, which implies (II).

In one spatial dimension, we also have the Sobolev embedding from H^2 to C^1. Indeed, we can use this to show that solutions are in C^2 for $n = 1$. First note that

$$((H\bar{u})_i)_x = \sum_{j=1}^{N}h_{ij}\frac{\partial K}{\partial x} * u_i,$$

and

$$((H\bar{u})_i)_{xx} = \sum_{j=1}^{N} h_{ij} \frac{\partial K}{\partial x} * \frac{\partial u_i}{\partial x},$$

which are both continuous. Therefore $[u_i((H\bar{u})_i)_x]_x = u_{ix}((H\bar{u})_i)_x + u_i((H\bar{u})_i)_{xx}$ is continuous. It follows from the mild formulation in Equation (3.1) that u_{it} is continuous. Consequently, $D_i u_{ixx} = u_{it} + [u_i((H\bar{u})_i)_x]_x$ is continuous, so u_i is in $C^2(\mathbb{T})$ (where $\mathbb{T} = [0, L]$ here, since $n = 1$). ∎

Lemma 3.9. *Consider the solution from Lemma 3.8 in one spatial dimension, so that* $n = 1$, $\mathbb{T} = [0, L]$, *and* $u \in C^1((0, T_*), L^2(\mathbb{T}))^N \cap C^0((0, T_*), C^2(\mathbb{T}))^N$. *Let* $u_0 \in C^2(\mathbb{T})^N$ *such that* $u_0(x) > 0$ *for* $x \in \mathbb{T}$. *Then* $u(x, t) > 0$ *for* $x \in \mathbb{T}$ *and* $t < T_*$.

Proof. We let $u = (u_1, \ldots, u_N)$ and work with each component separately. Assume that there is a first time $t_0 > 0$ such that the solution for u_i becomes zero at a point x_0. We can rule out the case that $u_i(t_0, x) \equiv 0$, since the system (2.3) conserves total mass. Then we have

$$u(t_0, x_0) = 0, \quad u_{ix}(t_0, x_0) = 0, \quad u_{ixx}(t_0, x_0) > 0, \quad u_{it}(t_0, x_0) < 0.$$

System (2.1) evaluated at (t_0, x_0) becomes

$$\begin{aligned} \underbrace{u_{it}(t_0, x_0)}_{<0} &= D_i u_{ixx}(t_0, x_0) - [u_i(t_0, x_0)((H\bar{u})_i(t_0, x_0))_x]_x \\ &= \underbrace{D_i u_{ixx}(t_0, x_0)}_{>0} - \Big[\underbrace{u_{ix}(t_0, x_0)}_{=0}((H\bar{u})_i(t_0, x_0))_x + \underbrace{u(t_0, x_0)}_{=0}(H\bar{u}(t_0, x_0))_{ixx}\Big], \end{aligned}$$

leading to a contradiction. Hence $u_i(x, t) > 0$. ∎

Theorem 3.10. *Let* $u_0 \in C^2(\mathbb{T})^N$ *such that* $u_0(x) > 0$ *for* $x \in \mathbb{T}$. *Then the solution from Lemma 3.8 is global in time (i.e.* $T_* = \infty$*) when working in one spatial dimension (*$n = 1$*).*

Proof. Recall that if $T_* < \infty$ then $\|u\|_{L^1} \to \infty$ at some point in time and T_* defined as the earliest time at which $\|u\|_{L^1} = 2\|u_0\|_{L^1}$. Therefore $\|u\|_{L^1}$ will be strictly greater than $\|u_0\|_{L^1}$ for some $t_* \in (0, T_*)$. But, since $\int_{\mathbb{T}} u dx = \|u_0\|_{L^1}$ for all time, we have $\int_{\mathbb{T}} u(x, t_*) dx < \int_{\mathbb{T}} |u(x, t_*)| dx$, which implies that there must be some x such that $u(x, t_*) < 0$, contradicting positivity (Lemma 3.9). Thus we must have $T_* = \infty$ and solutions are global in time. ∎

4. Numerics. In this section we describe a method to solve System (2.1) numerically, based on the general class of spectral methods [15]. For simplicity, we focus on simulations within 1D domains. However, this procedure may be also extended to any spatial dimension. Although our analytic results rely on the averaging kernel, K, being twice differentiable, our numerical method does not rely on this constraint. Since the study of [54] used a top-hat kernel (which is not differentiable), we demonstrate our method using this kernel as well as an example twice-differentiable kernel.

The leading idea behind a spectral method is to write the solution of a PDE as a sum of smooth basis functions with time dependent coefficients. By substituting this expansion in the PDE, we obtain a system of ordinary differential equations (ODEs), which can be solved using any numerical method for ODEs [13].

In the previous section we showed that, under the hypothesis of Lemma 3.8, any solution $u(x,t)$ to System (2.1) is C^2-smooth, so it is possible to expand it as

$$u(x,t) = \sum_{h=-\infty}^{\infty} \hat{u}_h(t)\phi_h(x),$$

where the coefficients $\hat{u}_h$ are computed by using the global behaviour of the function u and $\{\phi_h\}_h$ is a complete set of orthogonal smooth functions.

Since System (2.1) is periodic in space with period L, we adopt the Fourier basis as complete set of orthogonal functions and expand each component of the solution $u = (u_1, \dots, u_N)$ as

$$u_j(x,t) = \sum_{h=-\infty}^{\infty} \hat{u}_{jh}(t) e^{\frac{2\pi i}{L}hx}, \text{ for } j = 1, \dots, N, \tag{4.1}$$

where $\hat{u}_{jh}(t) = \frac{1}{L}\int_0^L u_j(x,t)e^{-\frac{2\pi i}{L}hx}dx$ are the Fourier coefficients, which represent the solution in the frequency space.

One of the advantages of working with the Fourier expansion is that the operation of derivation becomes particularly simple if performed in the frequency space. Indeed, differentiating Equation (4.1), we find

$$\partial_x u_j(x,t) = \sum_{h=-\infty}^{\infty} \frac{2\pi i}{L} h \hat{u}_{jh}(t) e^{\frac{2\pi i}{L}hx}, \text{ for } j = 1, \dots, N, \tag{4.2}$$

we see that the Fourier coefficients of the derivative are obtained by multiplying each $\hat{u}_{jh}$ by the term $\frac{2\pi i}{L}h$.

Another important property of the Fourier transform, particularly useful in our case, is that the convolution in the physical space is equivalent to a multiplication in the frequency space. Indeed, the Convolution Theorem states that the convolution between two functions $f(x) = \sum_{h=-\infty}^{\infty} \hat{f}_h e^{\frac{2\pi i}{L}hx}$ and $g(x) = \sum_{h=-\infty}^{\infty} \hat{g}_h e^{\frac{2\pi i}{L}hx}$ has the following Fourier expansion

$$f * g(x) = \sum_{h=-\infty}^{\infty} \hat{f}_h \hat{g}_h e^{\frac{2\pi i}{L}hx}. \tag{4.3}$$

Therefore, to solve numerically System (2.1) the operations of differentiations and convolution will be performed in the frequency space, while multiplications will be done in the physical space.

To implement our numerical method, we discretize both spatial and temporal domain, and consider the approximation of the solution $u(x,t)$ on the grid points $x_m = m\Delta x$ and $t^n = n\Delta t$, with $m \in \{0, 1, \dots, M-1\}$ and $n \in \mathbb{N}$. We define $U^n_{jm} = u_j(x_m, t^n)$. Then, in discrete space, the coefficients $\hat{u}_{jh}(t)$ of Equation (4.1) are replaced by

$$\hat{U}^n_{jh} = \frac{1}{M}\sum_{m=0}^{M-1} U^n_{jm} e^{-\frac{2\pi i}{M}hm}, \tag{4.4}$$

which represent the discrete Fourier transform (DFT) of $u_j(x,t)$.

The inverse discrete Fourier transform (IDFT), used to compute U^n_{jm} from $\hat{U}^n_{jh}$, is given by the formula

$$U^n_{jm} = \sum_{h=0}^{M-1} \hat{U}^n_{jh} e^{\frac{2\pi i}{M} hm}. \tag{4.5}$$

We can convert the solution from physical to frequency space, and vice versa, using the relations (4.4) and (4.5). However, we can speed the procedure up considerably by using a Fast Fourier Transform (FFT) algorithm, which reduces the number of computations from M^2 to $M \log M$ [55]. Analogously, an Inverse Fast Fourier Transform (IFFT) algorithm can be used to perform a fast backward Fourier transform from the frequency domain to the physical domain.

Let $\mathbf{U}^n_j = [U^n_{j0}, \ldots, U^n_{j(M-1)}]$, for $j = 1, \ldots, N$ and $\hat{\mathbf{U}}^n_j = [\hat{U}^n_{j0}, \ldots, \hat{U}^n_{j(M-1)}]$, for $j = 1, \ldots, N$, which represent the solution in the frequency domain at time $t = n\Delta t$. Then the algorithm for calculating the solution is as follows.

First, we calculate the non-local terms $\bar{\mathbf{U}}^n_j = K * \mathbf{U}^n_j$ by passing to the frequency domain and applying the Convolution Theorem (Equation (4.3)). We then stay in the frequency domain to calculate the derivative $\partial_x \bar{\mathbf{U}}^n_j$. Passing back to physical space, we calculate the product $\mathbf{U}^n_i \cdot \partial_x \bar{\mathbf{U}}^n_j$. Then the derivative of this product, $\partial_x(\mathbf{U}^n_i \cdot \partial \bar{\mathbf{U}}^n_j)$, is calculated in the frequency domain. This deals with the second term in our PDE (System 2.1). Finally, we calculate the diffusion term from System (2.1) by passing to frequency space.

This whole procedure results in defining a function, $f(\mathbf{U}^n_j)$, which is a discrete representation of the right-hand side of the PDE in System (2.1). Thus we have the following system of ODEs

$$\frac{d\mathbf{U}^n_j}{dt} = f(\mathbf{U}^n_j), \quad j = 1, \ldots, N, \tag{4.6}$$

which can be solved using any ODE solver. In particular, we used a Runge-Kutta scheme. To calculate the coefficients of Fourier transform and inverse Fourier transform, we used the `drealft` fast Fourier transform subroutine from [55]. This routine requires that the number of grid points must be a power of 2. We used the spatial domain $[0, 1]$ with 128 spatial grid points (so $\Delta x = 1/128$) and periodic boundary conditions.

For the spatial averaging kernel K, we used two different functions. The first is the von Mises distribution

$$K_a(x) = \frac{e^{a\cos(2\pi x)}}{I_0(a)}, \tag{4.7}$$

defined on $[-1/2, 1/2]$ (which is equivalent to $[0, 1]$ due to the periodic boundary conditions), where $I_0(a)$ is the modified Bessel function of order 0. This distribution both satisfies the periodic boundary conditions and is twice differentiable, as required by Lemma 3.2, Lemma 3.3, Lemma 3.4 and Lemma 3.7. We compare this with the following top-hat function

$\sigma = 0.1$, $\Delta t = 10^{-4}$	
$\mathcal{E}$	$t(s)$
$O(10^{-6})$	0.5216
$O(10^{-8})$	0.6043
$O(10^{-10})$	0.8522

$\sigma = 0.05$, $\Delta t = 10^{-4}$	
$\mathcal{E}$	$t(s)$
$O(10^{-6})$	0.2354
$O(10^{-8})$	0.4131
$O(10^{-10})$	0.6768

$\sigma = 0.025$, $\Delta t = 10^{-6}$	
$\mathcal{E}$	$t(s)$
$O(10^{-6})$	1.785
$O(10^{-8})$	3.918
$O(10^{-10})$	5.908

Table 1

Three tables showing numerical computation time, each for a different set of values of σ and Δt. The first column of each table contains the order of magnitude of the maximum distance between numerical solutions at times t and $t + \Delta t$ (first column) at the point when we stop the numerics. The second column shows the computational time in seconds to reach this point. The corresponding numerical simulations are shown in Figure 1

on $[-1/2, 1/2]$, used by [54]

$$K_\gamma(x) = \begin{cases} \frac{1}{2\gamma}, & -\gamma \le x \le \gamma, \\ \\ 0, & \text{otherwise.} \end{cases} \tag{4.8}$$

To compare numerical solutions with the two averaging kernels, K_a and K_γ, we use a common standard deviation

$$\sigma = \sqrt{\int_{-1/2}^{1/2} x^2 K(x)\mathrm{d}x - \left(\int_{-1/2}^{1/2} xK(x)\mathrm{d}x\right)^2}. \tag{4.9}$$

We implemented our algorithm in the C programming language and demonstrated it using the simple case of two interacting populations, u_1 and u_2. The numerical code is available at https://github.com/MathGiu/MS.

In Figure 1 we show the spatiotemporal evolution of the numerical solution, with $K = K_a$, for different values of the standard deviation σ. For $\sigma = 0.1$, we used a smooth random perturbation of the homogeneous steady state as initial condition. In this case, the solution appears to evolve towards a stationary state, and we stopped the numerics when the maximum distance between solutions at times t and $t + \Delta t$ is below 10^{-10}. This took about 0.8 seconds of computational time to reach (see Table 1). We then used this stationary state as initial condition for a simulation with $\sigma = 0.05$, whose spatiotemporal evolution is shown in the second line of Figure 1. As in the previous case, the solution appears to settle into a stationary state, which was used as initial condition to perform a simulation with $\sigma = 0.025$. We see that, as σ is decreased, the steady state solutions become increasingly flat-topped.

In each of these examples, $h_{ii} = 0$ for $i = 1, 2$. In this case, [54] showed that the system admits an energy functional which decreases over time, a feature that often accompanies systems that reach a stable steady state, and indeed this is what we observe in our numerics. However, if we drop the $h_{ii} = 0$ assumption, it is possible to observe patterns that exhibit oscillatory behaviour that does not appear to stabilise over time (Figure 2).

Comparing the numerical solutions obtained with the von Mises kernel (4.7) and top-hat kernel (4.8) for different values of σ, we see a good numerical agreement between numerical steady-state solutions (Figure 3). Hence, numerically, either choice is possible.

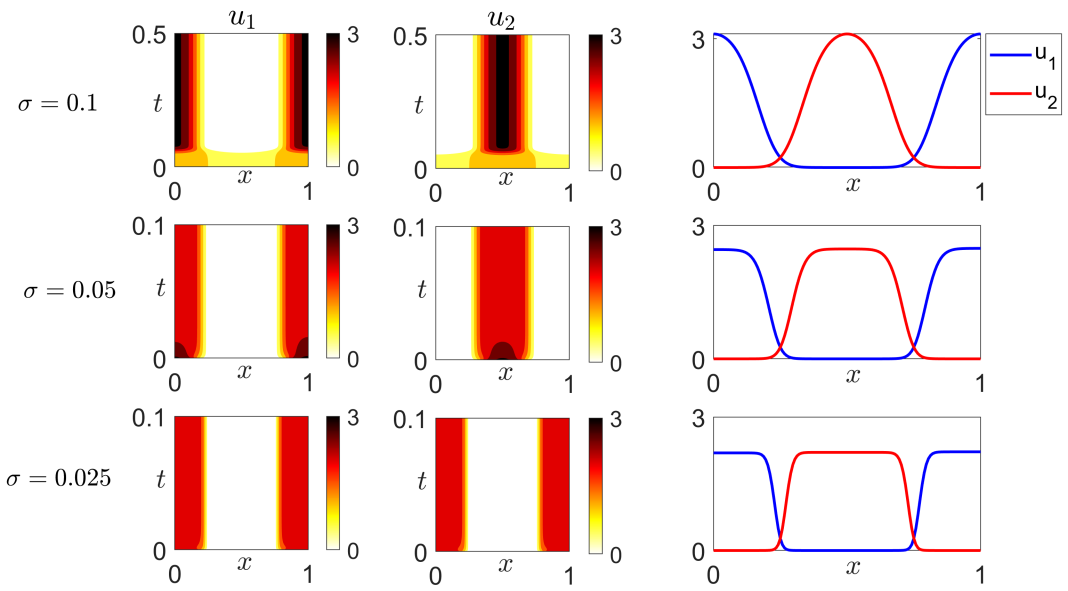

Figure 1. *Spatio temporal evolution of the numerical solution of (2.1) with $K = K_a$ defined in Equation (4.7), for different values of the standard deviation σ. On the right column: spatial profile of the numerical stationary solution. The parameter values are: $D_1 = D_2 = 1$, $h_{11} = h_{22} = 0$, $h_{12} = h_{21} = -2$. For $\sigma = 0.1$, $a = 3.225$; for $\sigma = 0.05$, $a = 10.664$; for $\sigma = 0.025$, $a = 41.01$.*

5. Discussion. The development of our model (Equation (1.2)) has been driven by the need to include non-local spatial terms into realistic models for organism interactions. However, when developing a new modelling framework, it is always a good idea to show that the model is well defined and biologically sensible, as we do here. In particular, it is important to identify the mathematical conditions that are needed to prove existence and uniqueness of solutions. In our case, for example, we find that the smoothness of the averaging kernel is essential to prove existence of classical solutions for the PDE model. This implies that our favorite choice, the indicator function on a ball of radius R, used by [54], is not included in the existence results. This is not a large restriction for the biology, since the indicator function can always be mollified (smoothed out) to obtain a regular kernel. However, it opens an interesting mathematical question to try to understand what goes wrong when the averaging kernel has jumps. In our case we cannot find a uniform L^∞ estimate for convolution with ∇K, which is an observation, but not an explanation of this limitation. In numerical simulations, we compare smooth and non-smooth averaging kernels and we see no appreciable difference. The difference is certainly much smaller than can ever be expected from errors that arise through empirical measurements of species distributions.

In our theory we consider a periodic domain, represented through the n-torus $\mathbb{T}$. Other

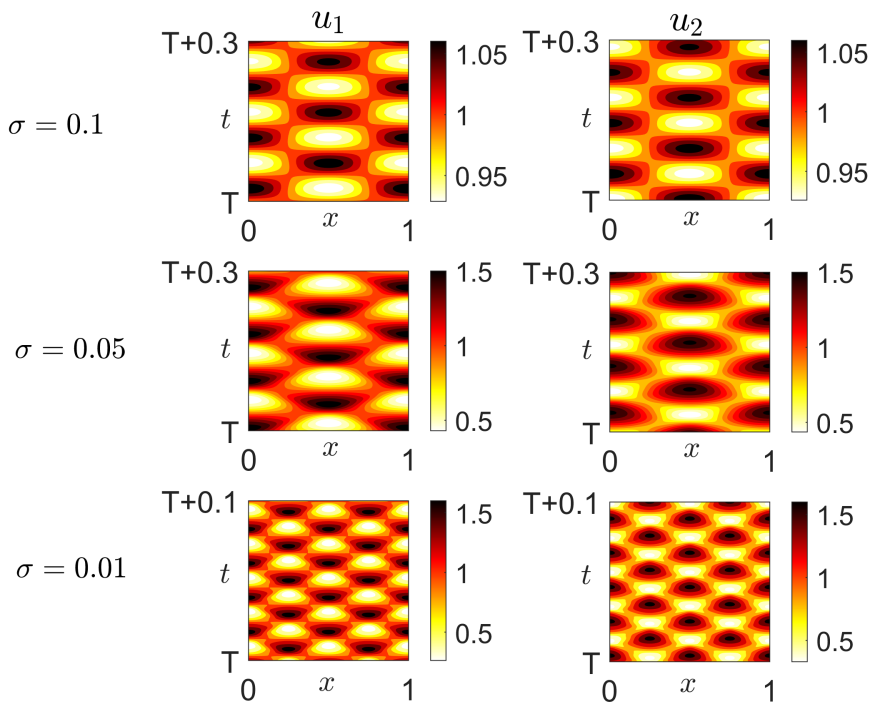

Figure 2. *Spatio temporal evolution of the numerical solution of* (2.1) *with* K *defined in Equation* (4.7)*, for different values of* σ*. The parameter values are:* $D_1 = D_2 = 1$*,* $h_{11} = h_{22} = h_{21} = 1.5$*,* $h_{12} = -1$*. For* $\sigma = 0.1$*,* $a = 3.1$*; for* $\sigma = 0.05$*,* $a = 10.5$*; for* $\sigma = 0.01$*,* $a = 250$*.*

domains with other boundary conditions can be studied with minimal modifications. The boundary conditions were essential to establish Lemma 3.5 about the regularity of the heat equation semigroup on $\mathbb{T}$. Similar regularity results are known for other boundary conditions [36, 40], and in those cases our method applies directly.

Non-local models for one or two species have been extensively studied before (see for example [18, 16] and the references that were mentioned in the Introduction). Our emphasis here is on a multiple species situation. This system was originally introduced in [54], in a slightly modified form, for the purposes of understanding the effect of between-population movements on the spatial structure of ecosystems, something generally ignored in species distribution modelling [24]. Understanding the spatial distribution of species has been named as one of the top five research fronts in ecology [57], so the model presented here has potential for giving insights into various important problems in biology where biotic interactions affect movement. These include, but are not limited to, the emergence of home range patterns [10], the geometry of selfish herds [30], the landscape of fear [37], and biological invasions [39].

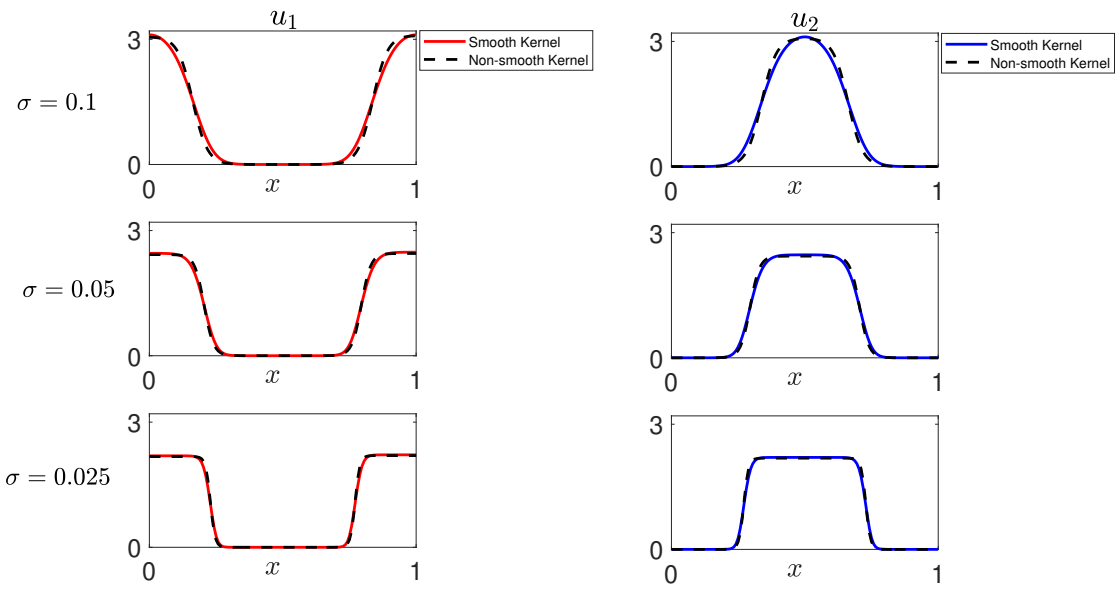

Figure 3. *Comparison between the spatial profiles of the stationary solutions obtained with the smooth kernel K (4.7) and the non-smooth kernel K_γ (4.8), for different values of the standard deviation σ. The parameter values are: $D_1 = D_2 = 1$, $h_{11} = h_{22} = 0$, $h_{12} = h_{21} = -2$. For $\sigma = 0.1$, $a = 3.225$ and $\gamma = 0.1732$. For $\sigma = 0.05$, $a = 10.664$ and $\gamma = 0.0866$. For $\sigma = 0.025$, $a = 41.01$ and $\gamma = 0.0433$.*

The study of [54] focused on pattern formation via the tools of linear stability, numerical bifurcation, and energy functional analysis. This study showed that the linear stability problem became ill-posed in the 'local limit', i.e. as K tends towards a Dirac delta function so that advection becomes local. Analogously, here we show that solutions exist for smooth K, but depend upon $\|\nabla K\|_\infty$ being finite, so will also break down if K is a Dirac delta function. This highlights the importance of non-locality in our advection term. Indeed, numerical simulations (e.g. Figure 1) suggest that, as K narrows (i.e. its standard deviation decreases), the maximum gradient of any non-trivial stable steady state increases. We conjecture that failure to include non-locality in the advection term (equivalently, setting K to be a Dirac delta function) will lead to gradient blow-up.

Our results, together with those of [54], suggest a rich variety of pattern formation properties in non-local multi-species advection-diffusion models. Here, specifically, we see two new features related to pattern formation. The first is the appearance of oscillatory solutions in two-species models, enabled by the inclusion of self-attractive terms. Second, we see that changing the width of spatial averaging, given by σ, can have a qualitative effect on the patterns that emerge (Figure 2). We have only scratched the surface here, in order to introduce our numerical method, the main purpose of this work being to establish existence of solutions.

Nonetheless, the ability to link underlying processes with emergent patterns is a principal question in biology [32, 19, 50], and the evident rich pattern formation properties of these models suggest this will be a formidable task for future work, building on the increasing literature in this area [52, 14, 17].

Acknowledgements We are grateful to two anonymous reviewers whose comments and suggestions helped improve the manuscript, and also Marco Sammartino who developed the preliminary coding structure on which our numerics were based.

REFERENCES

[1] M. B. Araujo and A. Guisan, *Five (or so) challenges for species distribution modelling*, Journal of biogeography, 33 (2006), pp. 1677–1688.
[2] N. J. Armstrong, K. J. Painter, and J. A. Sherratt, *A continuum approach to modelling cell–cell adhesion*, Journal of Theoretical Biology, 243 (2006), pp. 98–113.
[3] A. B. Barbaro, N. Rodriguez, H. Yoldaş, and N. Zamponi, *Analysis of a cross-diffusion model for rival gangs interaction in a city*, arXiv preprint arXiv:2009.04189, (2020).
[4] G. Bastille-Rousseau, D. L. Murray, J. A. Schaefer, M. A. Lewis, S. P. Mahoney, and J. R. Potts, *Spatial scales of habitat selection decisions: implications for telemetry-based movement modelling*, Ecography, 41 (2018), pp. 437–443.
[5] L. J. Beaumont, L. Hughes, and A. Pitman, *Why is the choice of future climate scenarios for species distribution modelling important?*, Ecology letters, 11 (2008), pp. 1135–1146.
[6] J. Bedrossian, N. Rodríguez, and A. L. Bertozzi, *Local and global well-posedness for aggregation equations and patlak–keller–segel models with degenerate diffusion*, Nonlinearity, 24 (2011), p. 1683.
[7] S. Benhamou, *Of scales and stationarity in animal movements*, Ecology Letters, 17 (2014), pp. 261–272.
[8] A. L. Bertozzi and T. Laurent, *Finite-time blow-up of solutions of an aggregation equation in R^n*, Communications in Mathematical Physics, 274 (2007), pp. 717–735.
[9] A. L. Bertozzi, T. Laurent, and J. Rosado, *l_p theory for the multidimensional aggregation equation*, Communications on Pure and Applied Mathematics, 64 (2011), pp. 45–83.
[10] L. Börger, B. D. Dalziel, and J. M. Fryxell, *Are there general mechanisms of animal home range behaviour? a review and prospects for future research*, Ecology Letters, 11 (2008), pp. 637–650.
[11] B. Briscoe, M. Lewis, and S. Parrish, *Home range formation in wolves due to scent marking*, Bull. Math. Biol., 64 (2002), pp. 261–284, https://doi.org/10.1006/bulm.2001.0273.
[12] M. Burger, R. Fetecau, and Y. Huang, *Stationary states and asymptotic behavior of aggregation models with nonlinear local repulsion*, SIAM Journal on Applied Dynamical Systems, 13 (2014), pp. 397–424.
[13] J. C. Butcher and N. Goodwin, *Numerical methods for ordinary differential equations*, vol. 2, Wiley Online Library, 2008.
[14] A. Buttenschön and T. Hillen, *Non-local Cell Adhesion Models: Symmetries and Bifurcations in 1-D*, Springer, New York, 2021.
[15] C. Canuto, M. Y. Hussaini, A. Quarteroni, and T. A. Zang, *Spectral methods: fundamentals in single domains*, Springer Science & Business Media, 2007.
[16] J. Carrillo, F. Hoffmann, and R. Eftimie, *Non-local kinetic and macroscopic models for self-organised animal aggregations*, Kinetic and Related Models, 8 (2015), p. 413, https://doi.org/10.3934/krm.2015.8.413, http://aimsciences.org//article/id/8639187c-b075-4a23-bba4-de4c12abfb7d.
[17] J. A. Carrillo, K. Craig, and Y. Yao, *Aggregation-diffusion equations: dynamics, asymptotics, and singular limits*, in Active Particles, Volume 2, Springer, 2019, pp. 65–108.
[18] J. A. Carrillo, Y. Huang, and M. Schmidtchen, *Zoology of a nonlocal cross-diffusion model for two species*, SIAM Journal on Applied Mathematics, 78 (2018), pp. 1078–1104.
[19] C. Cosner and R. Cantrell, *Spatial Ecology via Reaction-Diffusion Equations*, Wiley, Hoboken, 2003.
[20] K. Craig and A. Bertozzi, *A blob method for the aggregation equation*, Mathematics of computation,

85 (2016), pp. 1681–1717.
[21] F. Cucker and S. Smale, *Emergent behavior in flocks*, IEEE Trans. Automat. Control, 52 (2007), p. 852–862.
[22] M. G. Delgadino, X. Yan, and Y. Yao, *Uniqueness and nonuniqueness of steady states of aggregation-diffusion equations*, Communications on Pure and Applied Mathematics, (2019).
[23] J. Dolbeault and B. Perthame, *Optimal critical mass in the two dimensional keller–segel model in r^2*, Comptes Rendus Mathematique, 339 (2004), pp. 611–616.
[24] C. F. Dormann, M. Bobrowski, D. M. Dehling, D. J. Harris, F. Hartig, H. Lischke, M. D. Moretti, J. Pagel, S. Pinkert, M. Schleuning, et al., *Biotic interactions in species distribution modelling: 10 questions to guide interpretation and avoid false conclusions*, Global ecology and biogeography, 27 (2018), pp. 1004–1016.
[25] R. Eftimie, *Hyperbolic and kinetic models for self-organized biological aggregations and movement: a brief review*, Journal of Mathematical Biology, 65 (2012), pp. 35–75, https://doi.org/10.1007/s00285-011-0452-2, https://doi.org/10.1007/s00285-011-0452-2.
[26] R. Eftimie, J. Bramson, and D. Earn, *Interactions between the immune system and cancer: A brief review of non-spatial mathematical models*, Bulletin of Mathematical Biology, 73 (2011), pp. 2–32.
[27] R. Eftimie, G. de Vries, and M. Lewis, *Complex spatial group patterns result from different animal communication mechanisms.*, Proceedings of the National Academy of Sciences of the United States of America, 104 (2007), pp. 6974–6979, https://doi.org/10.1073/pnas.0611483104.
[28] J. H. Evers, R. C. Fetecau, and T. Kolokolnikov, *Equilibria for an aggregation model with two species*, SIAM Journal on Applied Dynamical Systems, 16 (2017), pp. 2287–2338.
[29] S. Fagioli and Y. Jaafra, *Multiple patterns formation for an aggregation/diffusion predator-prey system*, arXiv preprint arXiv:1904.05224, (2019).
[30] W. D. Hamilton, *Geometry for the selfish herd*, Journal of theoretical Biology, 31 (1971), pp. 295–311.
[31] T. Hillen and M. Lewis, *Mathematical ecology of cancer*, in Managing complexity, reducing perplexity. Modeling biological systems, J. Marsan and M. Delitala, eds., Springer, 2014, pp. 1–14.
[32] T. Hillen and K. Painter, *Transport and anisotropic diffusion models for movement in oriented habitats*, in Dispersal, Individual Movement and Spatial Ecology, M. A. Lewis, P. K. Maini, and S. V. Petrovskii, eds., Lecture Notes in Mathematics, Springer Berlin Heidelberg, 2013, pp. 177–222, https://doi.org/10.1007/978-3-642-35497-7_7, http://dx.doi.org/10.1007/978-3-642-35497-7_7.
[33] T. Hillen, K. Painter, and C. Schmeiser, *Global existence for chemotaxis with finite sampling radius*, Discr. Cont. Dyn. Syst. B, 7 (2007), pp. 125–144.
[34] T. Hillen and K. J. Painter, *A user's guide to pde models for chemotaxis*, Journal of mathematical biology, 58 (2009), pp. 183–217.
[35] F. James and N. Vauchelet, *Numerical methods for one-dimensional aggregation equations*, SIAM Journal on Numerical Analysis, 53 (2015), pp. 895–916.
[36] O. Ladyžhenskaja, V. Solonnikov, and N. Ural'ceva, *Linear and Quasilinear Equations of Parabolic Type*, AMS Providence, Rhode Island, 1968.
[37] J. W. Laundré, L. Hernández, and W. J. Ripple, *The landscape of fear: ecological implications of being afraid*, The Open Ecology Journal, 3 (2010).
[38] H. Levine, W. Rappel, and I. Cohen, *Self-organization in systems of self-propelled particles*, Phys. Rev. E, 63 (2000).
[39] M. A. Lewis, S. V. Petrovskii, and J. R. Potts, *The mathematics behind biological invasions*, vol. 44, Springer, 2016.
[40] G. Lieberman, *Second Order Parabolic Differential Equations*, World Scientific, Singapore, 1996.
[41] F. Lutscher, *Integrodifference Equations in Spatial Ecology*, Springer, New York, 2020.
[42] M. Marmion, M. Parviainen, M. Luoto, R. K. Heikkinen, and W. Thuiller, *Evaluation of consensus methods in predictive species distribution modelling*, Diversity and distributions, 15 (2009), pp. 59–69.
[43] R. Martinez-Garcia, C. H. Fleming, R. Seppelt, W. F. Fagan, and J. M. Calabrese, *How range residency and long-range perception change encounter rates*, Journal of theoretical biology, 498 (2020), p. 110267.
[44] A. Mogilner and L. Edelstein-Keshet, *A non-local model for a swarm*, Journal of Mathematical Biology, 38 (1999), pp. 534–570.

[45] J. D. Murray, *Mathematical biology II: Spatial models and biomedical applications*, Springer-Verlag New York Incorporated New York, 2003.
[46] A. Norberg, N. Abrego, F. G. Blanchet, F. R. Adler, B. J. Anderson, J. Anttila, M. B. Araújo, T. Dallas, D. Dunson, J. Elith, et al., *A comprehensive evaluation of predictive performance of 33 species distribution models at species and community levels*, Ecological Monographs, 89 (2019), p. e01370.
[47] A. Okubo and S. A. Levin, *Diffusion and ecological problems: modern perspectives*, vol. 14, Springer Science & Business Media, 2013.
[48] M. Osswald, E. Jung, F. Sahm, G. Solecki, V. Venkataramani, J. Blaes, S. Weil, H. Horstmann, B. Wiestler, M. Syed, L. Huang, M. Ratliff, K. Jazi, F. Kurz, T. Schmenger, D. Lemke, M. Gömmel, M. Pauli, Y. Liao, P. Häring, S. Pusch, V. Herl, C. Steinhï¿œuser, D. Krunic, M. Jarahian, H. Miletic, A. Berghoff, O. Griesbeck, G. Kalamakis, O. Garaschuk, M. Preusser, S. Weiss, H. Liu, S. Heiland, M. Platten, P. Huber, T. Kuner, A. von Deimling, W. Wick, and F. Winkler, *Brain tumour cells interconnect to a functional and resistant network*, Nature, 528 (2015), p. nature16071.
[49] K. Painter, J. Bloomfield, J. Sherratt, and A. Gerisch, *A nonlocal model for contact attraction and repulsion in heterogeneous cell populations*, Bulletin of Mathematical Biology, 77 (2015), pp. 1132–1165.
[50] J. Potts and K. J. Painter, *Stable steady-state solutions of some biological aggregation models*, SIAM J. Appl. Math., (in press).
[51] J. R. Potts, G. Bastille-Rousseau, D. L. Murray, J. A. Schaefer, and M. A. Lewis, *Predicting local and non-local effects of resources on animal space use using a mechanistic step selection model*, Methods in ecology and evolution, 5 (2014), pp. 253–262.
[52] J. R. Potts and M. A. Lewis, *How memory of direct animal interactions can lead to territorial pattern formation*, J Roy Soc Interface, (2016).
[53] J. R. Potts and M. A. Lewis, *Territorial pattern formation in the absence of an attractive potential*, J Math Biol, 72 (2016), pp. 25–46.
[54] J. R. Potts and M. A. Lewis, *Spatial memory and taxis-driven pattern formation in model ecosystems*, Bulletin of Mathematical Biology, 81 (2019), pp. 2725–2747, https://doi.org/10.1007/s11538-019-00626-9, https://doi.org/10.1007/s11538-019-00626-9.
[55] W. H. Press, H. William, S. A. Teukolsky, W. T. Vetterling, A. Saul, and B. P. Flannery, *Numerical recipes 3rd edition: The art of scientific computing*, Cambridge university press, 2007.
[56] V. Rai, *Spatial Ecology: Patterns and Processes*, Bentham Science, Sharja, 2018.
[57] I. W. Renner and D. I. Warton, *Equivalence of maxent and poisson point process models for species distribution modeling in ecology*, Biometrics, 69 (2013), pp. 274–281.
[58] L. Shahriyari, *A new hypothesis: some metastases are the result of inflammatory processes by adapted cells, especially adapted immune cells at sites of inflammation*, F1000 Research, 5 (2016). doi:10.12388/f1000research.8055.1.
[59] Q. Shi, J. Shi, and H. Wang, *Spatial movement with distributed memory*, Journal of Mathematical Biology, 82 (2021), pp. 1–32.
[60] M. Taylor, *Partial Differential Equations III*, Springer, New York, 1996.
[61] C. M. Topaz, A. L. Bertozzi, and M. A. Lewis, *A nonlocal continuum model for biological aggregation*, Bulletin of Mathematical Biology, 68 (2006), p. 1601.
[62] P. Turchin, *Population consequences of aggregative movement*, Journal of Animal Ecology, (1989), pp. 75–100.
[63] D. Villero, M. Pla, D. Camps, J. Ruiz-Olmo, and L. Brotons, *Integrating species distribution modelling into decision-making to inform conservation actions*, Biodiversity and Conservation, 26 (2017), pp. 251–271.
[64] N. E. Zimmermann, T. C. Edwards Jr, C. H. Graham, P. B. Pearman, and J.-C. Svenning, *New trends in species distribution modelling*, Ecography, 33 (2010), pp. 985–989.